ELSEVIER

Atmospheric Environment 38 (2004) 3241–3251

ATMOSPHERIC ENVIRONMENT

www.elsevier.com/locate/atmosenv

Seasonal variation of the particle size distribution of polycyclic aromatic hydrocarbons and of major aerosol species in Claremont, California

Antonio H. Miguel[a,*], Arantzazu Eiguren-Fernandez[a], Peter A. Jaques[a], John R. Froines[a], Bill L. Grant[a], Paul R. Mayo[a], Constantinos Sioutas[b]

[a] *Southern California Particle Center and Supersite, University of California, CHS 51.297, 650 Charles E. Young Drive South, Los Angeles, CA 90095-1772, USA*

[b] *Department of Civil and Environmental Engineering, University of Southern California, Los Angeles, CA 90089, USA*

Abstract

As part of the Southern California Particle Center and Supersite (SCPCS) activities, we measured, during all seasons, particle size distributions of 12 priority pollutant polycyclic aromatic hydrocarbons (PAHs), concurrently with elemental carbon (EC), organic carbon (OC), sulfate (SO_4^{2-}), and nitrate (NO_3^-) size distributions, from October 2001 to July 2002 in Claremont, CA, a receptor site located about 40 km downwind of central Los Angeles. Samples were collected approximately once every week, for 24-h periods, from midnight to midnight. MOUDI impactors collected samples at 30 LPM which were composited for analysis into monthly periods in three aerodynamic diameter size intervals, defined for the purpose of this work, as: 0–0.18 μm (ultrafine mode), 0.18–2.5 μm (accumulation mode), and 2.5–10 μm (coarse mode). For the monthly composites from October to February, the size distributions of the target PAHs are similar. However, from March to July, notable differences are observed: a significant fraction of the PAH mass is found in the coarse mode, as compared with the previous period. During the entire 1-year period, the form and shape of the EC size distributions did not vary much and are distinguished by prominent mass in the ultrafine and accumulation size mode. For the individual modes of the major species, the highest Pearson's correlation coefficients for the variation of temperature with species concentration were found in the ultrafine mode for both SO_4^{2-} (0.92) and EC (0.90), and in the coarse mode for both OC (0.85) and NO_3^- (0.54). High SO_4^{2-} correlations are consistent with increased gas-to-particle formation during the warmer months from (precursor) SO_2 emissions in the Los Angeles and Lon Beach seaport areas and, similarly for EC, increased atmospheric transport to Claremont as the season progresses from winter to summer. Although not statistically significant, the correlations were negative for the less volatile or particle phase group ($\log [p_L^o] \leqslant -3.22$), consistent with increased partitioning from the vapor phase with decreasing temperature.

Keywords: Polycyclic aromatic hydrocarbons; Elemental carbon; Organic carbon; Sulfate; Nitrate; Size distribution; Claremont; California

1. Introduction

During nearly a 1-year period, a comprehensive set of measurements was carried out in Claremont, California, as part of the Southern California Particle Center and Supersite (SCPCS) activities. This receptor area location is characterized by high concentrations of secondary air pollutant species including ozone, nitric acid, sulfate (SO_4^{2-}), nitrate NO_3^-, and particulate organic carbon (OC) (Blumenthal et al., 1987; Kim et al., 2000, 2002). Our recent studies conducted in Downey, a source area located near central Los Angeles, and in Rubidoux, a

*Corresponding author. Tel.: +310-825-9576; fax: +310-206-9903.

E-mail address: ahmiguel@ucla.edu (A.H. Miguel).

1352-2310/$ - see front matter © 2004 Elsevier Ltd. All rights reserved.
doi:10.1016/j.atmosenv.2004.03.008

receptor area 60 km downwind in the Los Angeles basin, showed that, during transport across the basin, after emission from combustion sources, the size distribution of PAHs undergoes changes from the ultrafine to the accumulation mode (Eiguren-Fernandez et al., 2003). Similar observations were reported by Venkataraman and Friedlander (1994), for other sites located downwind of the Los Angeles basin, and by Allen et al. (1996) for a rural location in Massachusetts. While the processes responsible for these size changes are not well understood, some hypotheses have been advanced and include the effects of major species present in the air parcel (e.g. EC, OC, SO_4^{2-}, and NO_3^-), aerosol dynamics, PAH phase partitioning, photochemical reactions, and meteorology.

PAHs emitted by vehicular emissions are associated with fine EC (Venkataraman and Friedlander, 1994; Miguel et al., 1998). EC concentrations in urban air are dominated by emissions from diesel engines including both on-highway and off-highway applications while EC + OC (total particulate carbon) result from the accumulation of small increments from a variety of emission source types such as gasoline and diesel powered highway vehicles, stationary source fuel oil and gas combustion, industrial processes, paved road dust, fireplaces, cigarettes and food cooking (Gray and Cass, 1998). Recent experiments carried out in the Caldecott tunnel (east of Berkeley, CA.) showed that, on a mass/volume of fuel basis, the contribution of EC by heavy-duty diesel vehicles is ca. 50-fold of that estimated for light-duty gasoline vehicles (Miguel et al., 1998).

Measurements of the seasonal variations of the PM_{10} size distribution of PAHs, concurrently with EC, OC, SO_4^{2-}, and NO_3^- size distributions in receptor areas may help improve our understanding of the processes that govern the observed shifts toward larger PAH size modes which occur during increased atmospheric transport. Knowledge of changes in particle size distributions is of paramount importance because it may modify their dry and wet deposition, atmospheric residence time, and deposition efficiency in the human respiratory system. Major objectives of the present 1-year study included: (i) Measurement of the seasonal effects on the size distribution of PAHs in a receptor site in the LA basin, located 40 km across from Central Los Angeles, and (ii), concurrent measurements of the size distribution of EC, OC, SO_4^{2-}, and NO_3^-, wind speed (WS), wind direction (WD), temperature (T) and relative humidity (RH) to evaluate their role on observed changes of PAH size distributions as they are transported across the Los Angeles basin to the inland valleys located eastward of downtown, which are considered receptor sites of the pollution produced in urban Los Angeles.

2. Experimental methods

2.1. Sample collection and sites

Sampling was carried out for 24-h periods approximately once every week from midnight to midnight, in Claremont, CA, from October 2001 to July 2002 (Fig. 1). At this downwind site, primary and secondary particulate matter (PM) are mixed with wind blown dust from the nearby deserts. A high fraction of PM2.5 mass at this location consists of labile species such as ammonium nitrate and semi-volatile organic compounds (Turpin and Huntzicker, 1994). In addition, PM originally emitted in urban Los Angeles is advected into the Claremont area after several hours of atmospheric transport (Wolf et al., 1991). Thus, we refer to the Claremont air pollution regime as a ''receptor'' area of the Los Angeles Basin. Samples were collected using a four- or five-stage Microorifice Uniform Deposit Impactors (MOUDI Model 110, MSP Corp., Minneapolis, MN). For analysis, monthly samples were composited into three aerodynamic diameter size intervals: 0–0.18 μm (ultrafine mode), 0.18–2.5 μm (accumulation mode), and 2.5–10 μm (coarse mode). For PAHs, EC, and OC quantification, samples were deposited on un-coated pre-baked aluminum foils (accumulation mode) and pre-baked quartz filters (coarse and ultrafine mode) using a MOUDI impactor. The use of quartz substrates for the coarse PM mode was preferred over aluminum in order to reduce potential particle bounce problems which would be more pronounced for coarse PM. Quartz filters used as impaction substrates have been shown to minimize particle bounce without affecting the cutpoint of the impactor (Chang et al., 1999, 2001). Another impactor used Teflon membrane filters (2 μm pore, PTFE, Gelman, Ann Arbor, MI) in all stages to collect particles for measurement of SO_4^{2-} and NO_3 by ion chromatography. The monthly composites of three size bins were necessary to collect enough target PAH and mass for quantification.

2.2. Meteorology measurements

WS and WD were recorded using a Met-One Instruments Inc. (OR) model 034A system, and RH and T using a Vaisala Inc. (MA) model HMP45A unit. The meteorological data collected were averaged by day and month to coincide with the particulate matter sampling scheme.

2.3. PAHs, sulfate and nitrate quantification

Details of the procedure for PAH quantification are described elsewhere (Eiguren-Fernandez and Miguel, 2003). Briefly, the impaction substrates corresponding to each size interval monthly composite were ultrasonically

Fig. 1. Map of the Los Angeles Basin with major freeways indicating the location of the Claremont study site.

extracted with dichloromethane (DCM) and analyzed by HPLC-fluorescence. NIST SRM 1649a standard was used as positive control. Standard deviations for the target PAHs running triplicate analysis of the as positive control averaged 8.0% and ranged from 3.8% to 15%. Likewise, sulfate and nitrate were extracted ultrasonically for 30 min with Milli-Q deionized water and quantified using a Dionex DX-100 ion chromatograph equipped with an AS4A anion analytical column and AG4A guard column, by elution with sodium carbonate/bicarbonate buffer. NIST traceable standards (SPEX Industries, Edison, NJ) were used as positive control for sulfate (cat AS-SO49-2y) and nitrate (cat #AS-NO39-2y). Standard deviation for duplicate determinations of both anions ranged from 0.2% to 7.5%. For all species, amounts found in the blanks were subtracted from the sample values.

3. Results and discussion

3.1. General

The main purpose of this study was the measurement of the seasonal variations of the size distribution of PAHs in Claremont during a 1-year period. EC, OC, SO_4^{2-}, and NO_3^- size distributions were measured concurrently to help us better understand the processes that may contribute to the observed changes in the size distribution of the target PAHs. It was not intended to be an evaluation of the partitioning phenomena that govern the atmospheric behavior of PAHs, nor the mechanisms that lead to the size distribution of the major species reported in this study. For recent detailed descriptions of these processes, the reader is referred to articles in the literature and references therein (Griffin et al., 2003; Seinfeld et al., 2001; Mader and Pankow, 2001; Hughes et al., 2002; Lohmann et al., 2000; Junge, 1977; Liang et al., 1997; Odum et al., 1996; Saxena and Hildemann, 1996; Pankow, 1987, 1994; Cotham and Bidleman, 1995).

3.2. General meteorology trends at Claremont during the sampling period

Table 1 lists daily temperature (T), relative humidity (RH), and wind speed (WS) averaged across the several days of PM sampling for each month presented, and reflect their respective dominant trends. Wind direction (WD) is determined by qualitative observation of wind rose plots generated with hourly data from the PM sample days of a given month. The results show that WS and WD in Claremont vary with season. WS peaks between March and July, and predominantly originates from the west and southwest. This is expected to affect the transport of fine PM from freeways to the south

Table 1
Mean temperature, relative humidity, wind direction, and wind speed measured in Claremont during the sampling periods

	Temp. (°C)	R.H. (%)	WD Predominant quadrant	WS Average ±S.D. (mph)
Oct 01	19.4	64.0	SW	3.2±1.5
Nov 01	14.7	44.7	SW & NE	3.4±1.9
Dec 01	10.6	45.7	SW & SE	2.7±0.7
Jan 02	12.4	38.8	SW & SE	3.0±1.0
Feb 02	15.6	33.7	S	3.2±1.4
Mar 02	15.9	49.9	W–SW	3.7±1.8
Apr 02	15.6	52.0	W–SW	3.9±1.9
May 02	19.3	52.0	W–SW	3.9±2.3
June 02	21.7	55.6	W–SW	3.7±2.1
July 02	25.6	46.3	W–SW	3.8±2.1

S.D. = standard deviation.

(210, 10, and 605), and likely more distant freeways to the west and southwest (110, 710, and 405) towards the monitoring site at Claremont (see map, Fig. 1). Additionally, during the long summer season, greater mid-day wind speeds and a higher mixing layer is expected to disperse transported PM concentrations. A more detailed observation of the data provide greater detail of diurnal wind patterns that may help explain some of the seasonal PAH trends observed in this study. For example, during the summer months, and more persistently during June and July, winds come predominantly from the south–west and west–south–west, starting at about 7–8 am, through about 8–10 pm, and increase in velocity through mid-day to as high as 8–10 mph. In the evening, the wind origin reverses direction rather rapidly, shifting from the north–north–west, peaking at about 2–3 mph to become much more stable. In contrast, during the winter, especially December through February, the morning wind varies from the South and West, and the morning shift from the North to the South starts later than in the summer (about 10 am to noon), persisting to between 5 and 7 pm. The winter daytime wind speed is lower and less variable than in the summer, while the evening north–north–west winds persist longer, and tend to be slightly faster, peaking between 3 and 5 mph. Seasonal temperature and relative humidity effects are related to the meteorological patterns. The average monthly RH is generally lowest in the colder winter months and is especially low during January and February at 39% and 34%, respectively, likely due to the greater contribution of persistent evening winds from the deserts to the North. Relative to the summer months, the more stable air mass and lower mixing heights experienced in the winter should reduce the rates of aerosol dispersion. The effects of temperature on the PAH size distributions reported in this study are discussed in Section 3.5.

3.3. PAHs and EC size distributions

The target PAHs were grouped according to their sub-cooled vapor pressure, p_L^o (Pa). The group of semivolatile PAH (log $[p_L^o]$ from −0.95 to −2.06) includes PHE, ANT, PYR, and FLT. The group of less volatile and particle phase PAHs (log $[p_L^o]$ from −3.22 to −7.04) includes BAA, CRY, BGP, BAP, BBF, BKF, DBA and IND. Their names, MW, and individual sub-cooled liquid vapor pressures are listed in Table 2.

PAHs (by vapor pressure group) and EC size distributions and total species mass (C) measured in Claremont from November 2001 to July 2002, are presented in Fig. 2. For the monthly composites from October to February, the size distribution of PAHs, in either group, is similar. During the entire period, the form and shape of the EC size distributions did not vary much and are distinguished by prominent accumulation (50% of the mass) and ultrafine (43% of the mass) modes. Coarse EC represented only ca. 7% of the total EC mass. The total EC concentrations (C) continuously decrease from October to January, and then increase from March to June. For the entire period, for the BAA–IND and the PHE–FLT group, respectively, the accumulation mode accounted for 42% and 46% of the mass, the ultrafine mode with 40% and 30%, and the coarse mode with 19% and 24% of the mass.

From March to July, notable differences are observed in the PAH distributions in both PAH groups: A significant fraction of the PAH mass is observed in the coarse mode, as compared with the previous period. The EC/TC ratios reported by Schauer (2003) for wood combustion products (0.02–0.10) and for motor vehicle emissions (0.50–0.80) suggest that, on a relative basis, larger amounts of PAHs (compared with EC) might be expected to be emitted during the winter and spring

Table 2
PAH codes, molecular weight, and subcooled liquid vapor pressure (Pa) at 293 K

PAH	Code	MW	$(\log p_L^o)$[a]
Phenanthrene	PHE	178	−0.95
Anthracene	ANT	178	−1.11
Pyrene	PYR	202	−1.92
Fluoranthene	FLT	202	−2.06
Benz[*a*]anthracene	BAA	228	−3.22
Chrysene	CRY	228	−3.97
Benzo[*ghi*]perylene	BGP	276	−4.65
Benzo[*a*]pyrene	BAP	252	−4.67
Benzo[*b*]fluoranthene	BBF	252	−4.99
Benzo[*k*]fluoranthene	BKF	252	−5.39
Dibenz[*a,h*]anthracene	DBA	278	−7.04
Indeno[1,2,3-*cd*]pyrene	IND	276	[b]

[a] Data from Peters et al. (2000), p_L^o in (Pa).
[b] Not available.

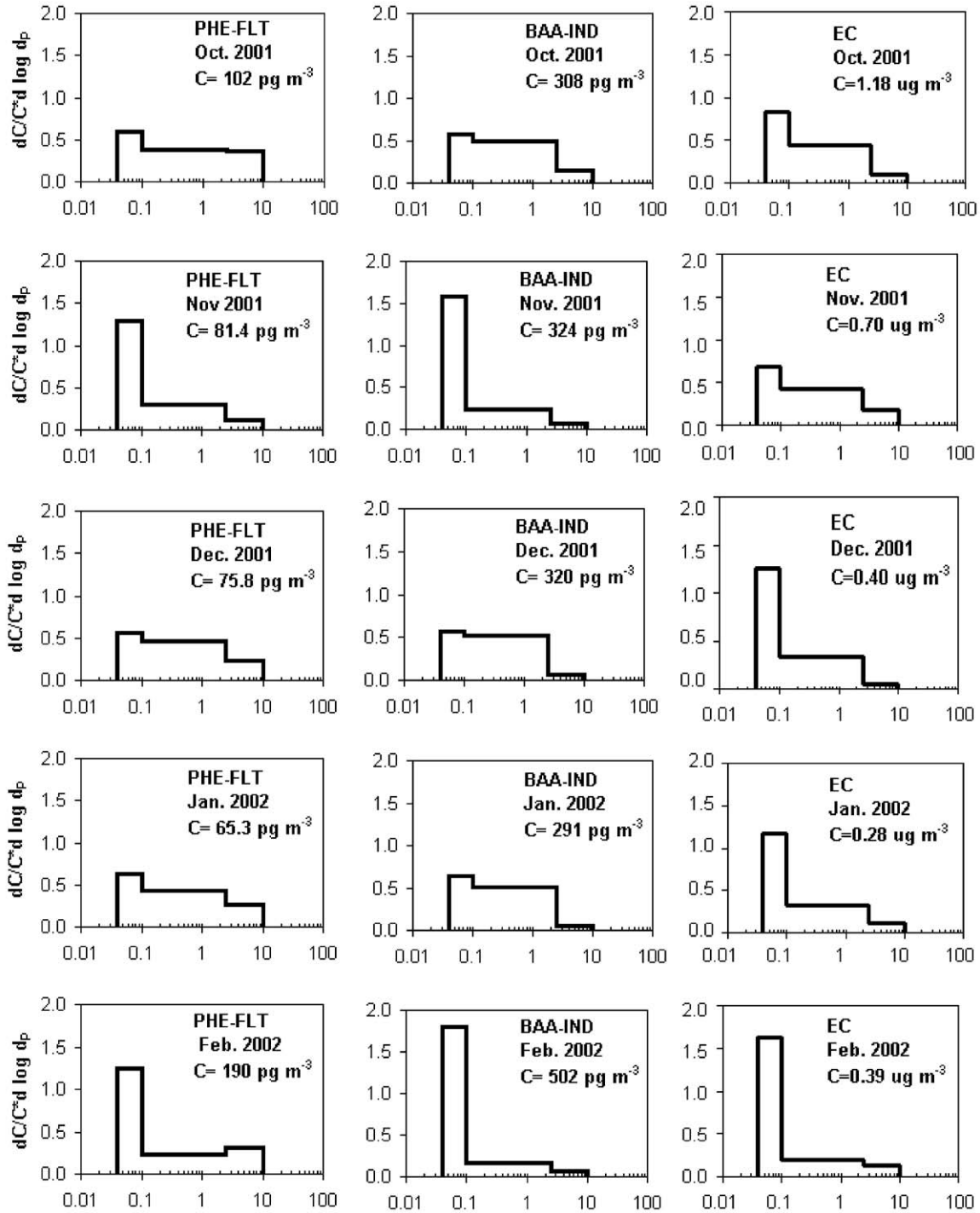

Fig. 2. Monthly particle size distribution of PAHs and EC composites measured in Claremont. Each mode corresponds to particles with aerodynamic diameter between 0 and 0.18 μm (ultrafine mode), 0.18 and 2.5 μm (accumulation mode), and 2.5 and 10 μm (coarse mode). The group of semivolatile PAH (log $[p_L^o]$ from −0.95 to −2.06) includes PHE, ANT, PYR, and FLT. The group of less volatile and particle phase PAHs (log $[p_L^o]$ from −3.22 to −7.04) includes BAA, CRY, BGP, BAP, BBF, BKF, DBA and IND.

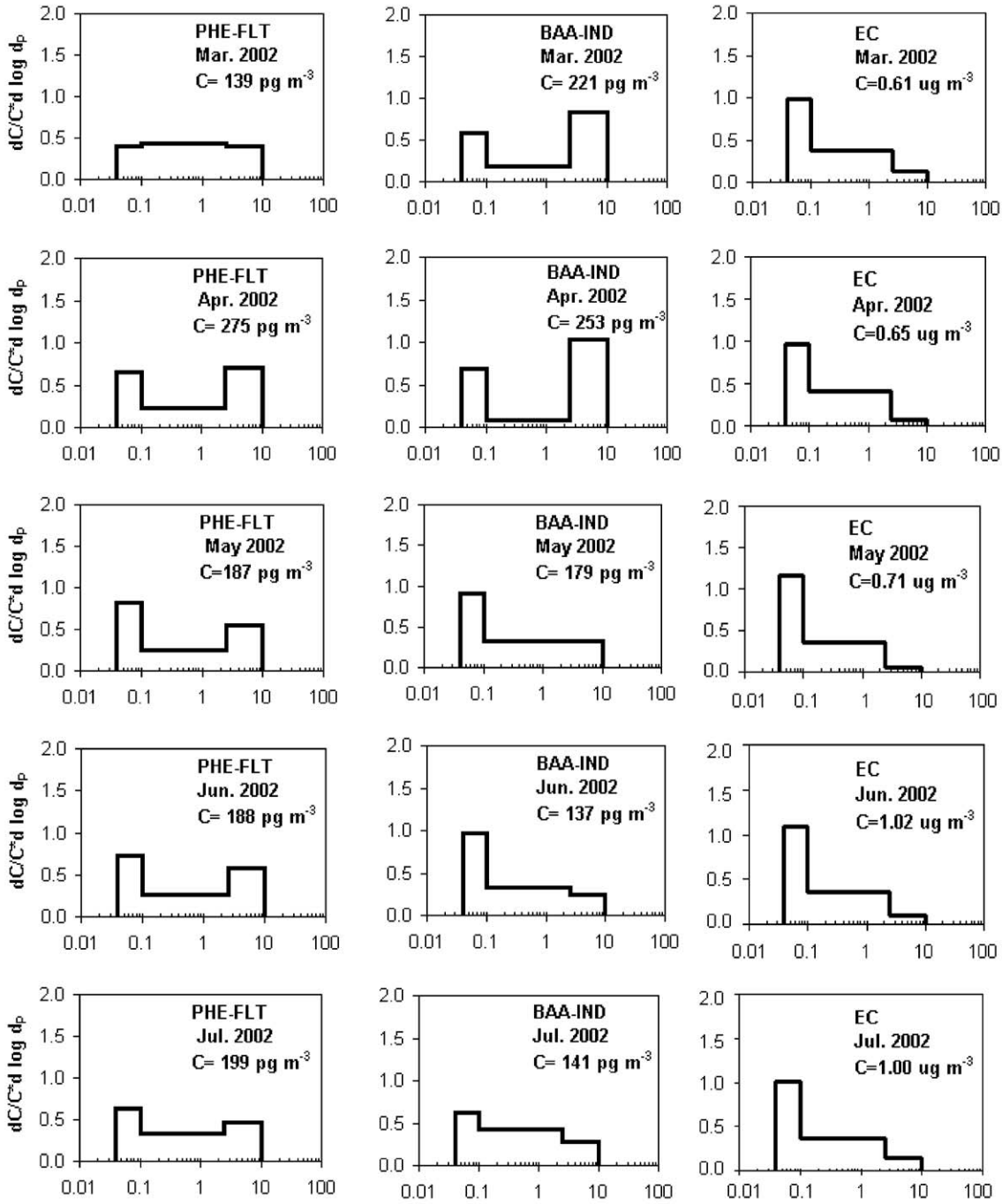

Fig. 2 (*continued*).

from wood combustion. Retene, a semi-volatile PAH that predominately originates from the combustion of wood from conifer trees, was found to be present at significant levels during the winter and spring periods (but not during summer and fall!) in Upland, located ~5 km southeast of Claremont (Manchester-Neesvig et al., 2003). While wood combustion clearly affects PAH levels, the reasons for the observed increased coarse mode PAHs from March to July remain unclear. Chemical reactions provide a mechanism that may

contribute with the loss of ultrafine PAHs. Samples collected in the Caldecott Tunnel show that the target PAHs have a major peak in the ultrafine mode (Miguel et al., 1998; Marr et al., 1999). As ultrafine PAHs are thought to be adsorbed on elemental carbon (or soot), thermodynamics would favor their reaction in this mode, leading to relatively larger accumulation modes. Allen et al. (1996) reported that in rural samples collected in Massachusetts, low and high MW PAHs were associated with both the fine and coarse aerosols and attributed it to slow mass transfer by vaporization and condensation. A similar absorption model was developed by Venkataraman et al. (1999), suggesting that the predominance of semi-volatile PAHs in the accumulation mode results from their volatilization from ultrafine particles (Kelvin effect), and subsequent partitioning to the accumulation mode where secondary organic aerosol constituents are available. The atmospheric lifetimes (2.9–11 h) calculated by Arey (1998) for day-time gas-phase reactions of OH with target PAHs in the more volatile group allow for reactions to occur during transport (Arey et al., 1989). For nighttime gas-phase reactions of NO_3 with these PAHs, the atmospheric lifetimes range from days to years (Arey, 1998). Further evidence of photolysis of PAHs on atmospheric soot particles with respect to humidity, sunlight, and temperature, was shown by Kamens et al. (1988). Therefore, aerosol dynamics, chemical reactions, and air parcel dilution contribute to decreased concentrations of particle bound PAHs during transport. For instance, Venkataraman and Friedlander (1994) reported that the shift of mass towards the secondary mode by atmospheric processes lowers the average deposition velocity by factors of 1.5–3.5, leading to longer residence times in the atmosphere. The effects of temperature on the PAH size distributions are discussed in Section 3.5.

3.4. Sulfate, nitrate and OC size distributions

SO_4^{2-}, NO_3^-, and OC size distributions and total species mass (C) for monthly composites measured concurrently are presented in Fig. 3. For the yearly SO_4^{2-} composites, the accumulation, coarse and ultrafine modes contained, respectively, 77%, 19% and 4% of mass. NO_3^- size distributions varied markedly over the entire period. From October to February, the mass in the accumulation and coarse modes contained, respectively, 78% and 22% its total mass, while from March to July, they represented 45% and 55% of the total NO_3^- mass. Similar SO_4^{2-} and NO_3^- size distributions were reported by Wall et al. (1988) for Claremont. In their study, SO_4^{2-} and NO_3^- showed two modes in the 0.1–1.0 μm size range, and a third mode over 1 μm (coarse mode). The mode around 0.2 μm (condensation) results from the condensation of secondary organic aerosol components from the gas-phase (Seinfeld and Pandis, 1998), while the droplet mode around 0.7 μm is attributed to heterogeneous, aqueous-phase reactions (Meng and Seinfeld, 1994). Coarse mode nitrate may result from the reaction of HNO_3 with sea salt and crustal material (Seinfeld and Pandis, 1998). Ammonia concentrations from a nearby area of large livestock and agricultural activities, contribute with increased concentrations of nitrate measured by Hughes et al. (2000) downwind in Riverside, and constitute a major source of precursor of nitrate. The largest effect of nitric-acid produced coarse nitrate is expected to occur during the summer, due to increased photochemical activity.

For all OC monthly composites, 60%, 24% and 16% of the mass measured were, respectively, in the accumulation, ultrafine, and coarse modes (Fig. 3). During the entire period, the fraction of mass in the coarse mode was much higher for OC, as compared with EC. In fact, the size distribution of the OC composite measured in May clearly shows a coarse mode (Fig. 3). Collection of OC on quartz fiber filters has been shown to produce positive sampling artifacts (Lewtas et al., 2001; McMurry and Zhang, 1989; Turpin and Huntzicker, 1994) due to adsorption of gas-phase organics onto the filter. For an average OC concentration of 6 $\mu g\,cm^{-3}$, measured in nearby Glendora, Turpin and Huntzicker (1994) reported that about 30% of the organic material deposited on a filter was attributed to vapor adsorption. For this reason, the OC mass observed in the ultrafine mode (Fig. 3) could be 30% lower when correcting for this sampling artifact. Even after considering this correction, a substantial fraction of the OC mass (~23%) would still be found in the ultrafine mode in the May and July composites.

3.5. Correlations of ambient temperatures with PAHs, EC, OC, SO_4^{2-}, and NO_3^- size distributions

Table 3 shows the Pearson's correlation coefficients (r) calculated for each mode and the total mass (C) of each measured species. For the individual modes of the major species measured, the highest correlations were found in the ultrafine mode for SO_4^{2-} (0.92) and EC (0.90), and in the coarse mode for OC (0.85) and NO_3^- (0.54). Except for NO_3^- (−0.29), the correlations found with the major species were all positive, consistent with increased rates of formation with increased temperature (SO_4^{2-}), atmospheric transport (EC, OC, SO_4^{2-}) to Claremont as the season progresses from winter to summertime. For NO_3^- in the accumulation PM mode, which is mostly associated with ammonium nitrate, as opposed to the sodium nitrate which predominates the coarse mode, the reduced concentrations observed during the warmer period are also consistent with the increase in the value of the dissociation constant of the

solid–gas equilibrium between particulate ammonium nitrate and gas-phase nitric acid and ammonia (Wexler and Seinfeld, 1991; Mozurkewich, 1993).

For PAHs, the highest correlations for individual modes were found in the accumulation mode for both the PHE–FLT group (0.60), and the BAA–IND group (−0.47). Although not statistically significant, the correlations found for all PAHs in the less volatile and particle phase group (BAA–IND) were all negative, consistent with increased vapor sorption in the particulate phase with decreasing temperature. For the more volatile group (PHE–FLT) all correlations were positive. PAHs in this group have vapor pressures that are between one and five orders of magnitude higher, and

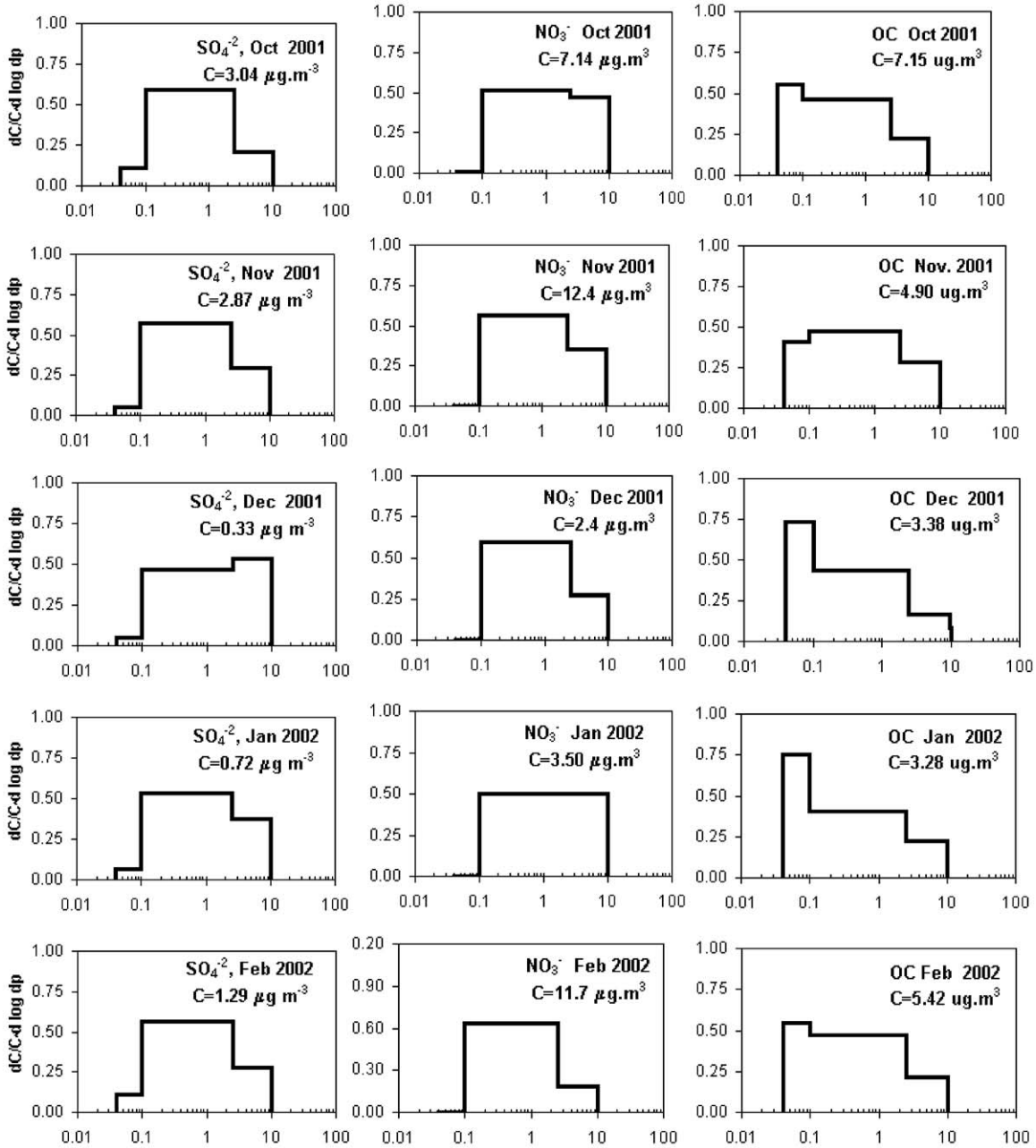

Fig. 3. Monthly particle size distributions of sulfate, nitrate and OC composites measured in Claremont. Each mode corresponds to particles with aerodynamic diameter between 0 and 0.18 μm (ultrafine mode), 0.18 and 2.5 μm (accumulation mode), and 2.5 and 10 μm (coarse mode).

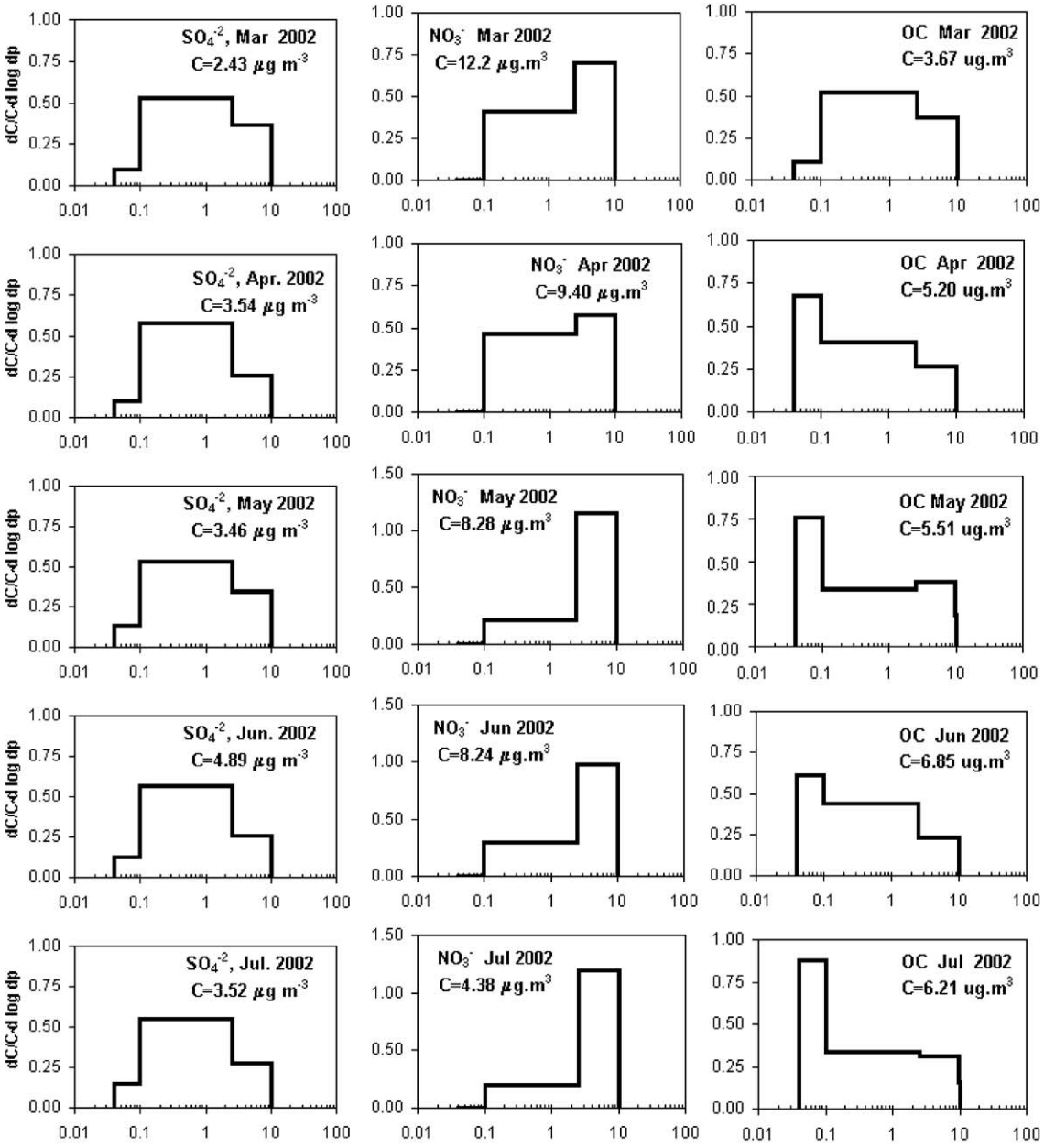

Fig. 3 (*continued*).

thus are found mostly in the vapor phase. Conversely, PAH in the BAA–IND group are found predominantly in the particle phase. Pankow and Bidleman (1992) reported that compounds found mostly in the vapor phase have low vapor/particle partition coefficients and it is therefore expected that their vapor/particle distribution will be less affected by temperature than compounds found mostly in the particle phase.

4. Conclusions

Seasonal effects on the size distribution of PAHs, EC, OC, SO_4^{2-}, and NO_3^- are presented in this study. While the size distributions of the target PAHs are similar from October to February showing significant ultrafine and accumulation modes, notable differences are observed from March to July when a significant fraction of the

Table 3
Pearson coefficient (r) for the correlation of ambient temperature with PAH group, EC, OC, SO_4^{2-}, and NO_3^- concentration in each mode, and for the total species mass (C).

Group or species	Ultrafine	Accumulation	Coarse	C
PHE–FLT[a]	0.30	**0.60**	0.42	0.50
BAA–IND[b]	−0.29	**−0.47**	−0.05	−0.61
EC	**0.90**	0.69	0.68	0.81
OC	0.73	0.51	**0.85**	0.80
SO_4^{2-}	**0.92**	0.77	0.71	0.78
NO_3^-	0.18	−0.29	**0.54**	0.02

The highest correlation values for each mode are shown in bold.
[a] $\log [p_L^o] \geqslant -2.06$.
[b] $\log [p_L^o] \leqslant -3.22$.

PAH mass is found in the coarse mode. While the reasons for these differences are not well understood, changes observed in wind speed and direction from the first to the second period appear to play a role. Contrasting these findings, during the entire study period, the form and shape of the EC size distributions did not vary much and are distinguished by prominent mass in the ultrafine and accumulation size modes. For individual modes of the major species measured, the highest Pearson's correlation coefficients for the variation of temperature with species concentration were found in the ultrafine mode for both SO_4^{2-} (0.92) and EC (0.90), and in the coarse mode for both OC (0.85) and NO_3^- (0.54). High SO_4^{2-} correlations are consistent with increased gas-to-particle formation, and atmospheric transport of sulfate to Claremont from precursor SO_2 ship emissions in the ports of Los Angeles and Long Beach as the season progresses from winter to summer. Relative to the summer months, the more stable air mass and lower mixing heights experienced in the winter contribute to reduce aerosol dispersion.

Although not statistically significant, correlations of decreasing temperature with increasing concentration of PAHs in the less volatile or particle phase group ($\log [p_L^o] \leqslant -3.22$) are consistent with increased partitioning from the vapor phase and increased photostability during the winter. As the temperature rises from March to July, the fraction of the NO_3^- mass in the coarse mode increases significantly, consistent with increased photochemical production of HNO_3 combined with increased atmospheric transport to Claremont of sea salt, ammonia, and crustal material precursors.

Acknowledgements

This research was supported by the Southern California Particle Center and Supersite (SCPCS). Although the research described in this article has been funded wholly or in part by the United States Environmental Protection Agency through Grants #R827352-01-0 and CR-82805901 to UCLA, it has not been subjected to the Agency's required peer and policy review and therefore does not necessarily reflect the views of the Agency and no official endorsement should be inferred. We thank Karen R. Anderson, Los Amigos Research Education Institute for IC analyses.

References

Allen, J.O., Dookeran, K.M., Smith, K.A., Sarofim, A.F., Taghizadeh, K., Lafleur, A.L., 1996. Measurement of polycyclic aromatic hydrocarbons associated with size-segregated atmospheric aerosols in Massachusetts. Environmental Science and Technology. 30, 1023–1031.

Arey, J., 1998. Atmospheric reactions of PAHs including formation of nitroarenes. In: Neilson, A.H. (Ed.) The Handbook of Environmental Chemistry, PAHs and Related Compounds, Vol. 3, Part I, Springer, Berlin, pp. 347–385.

Arey, J., Atkinson, R., Zielinska, B., McElroy, P.A., 1989. Diurnal concentrations of volatile polycyclic aromatic hydrocarbons and nitroarenes during a photochemical air pollution episode in Glendora, California. Environmental Science and Technology 23, 321–327.

Blumenthal, D.L., Watson, J.G., Roberts, P.T., 1987. Southern California Air Quality Study (SCAQS) Program Plan (prepared for the California Air Resources Board). Sonoma Technology Inc., Santa Rosa, CA.

Chang, M., Kim, S., Sioutas, C., 1999. Experimental studies on particle impaction and bounce: effects of substrate design and material. Atmospheric Environment 15, 2313–2323.

Chang, M.C., Sioutas, C., Fokkens, P.B., Cassee, F.R., 2001. Field evaluation of a mobile high-capacity particle size classifier (HCPSC) for separate collection of coarse, fine and ultrafine particles. Journal of Aerosol Science 32, 139–156.

Cotham, W.E., Bidleman, T.F., 1995. Polycyclic aromatic hydrocarbons and polychlorinated-biphenyls in air at an urban and rural site near Lake Michigan. Environmental Science and Technology 29, 2782–2789.

Eiguren-Fernandez, A., Miguel, A.H., 2003. Determination of semi-volatile and particulate polycyclic aromatic hydrocarbons in SRM 1649a and PM2.5 samples by HPLC-fluorescence. Polycyclic Aromatic Compounds 23, 193–205.

Eiguren-Fernandez, A., Miguel, A.H., Jaques, P., Sioutas, C., 2003. Evaluation of a denuder-MOUDI-PUF sampling system to measure the size distribution of semivolatile polycyclic aromatic hydrocarbons in the atmosphere. Aerosol Science and Technology 37, 201–209.

Gray, H.A., Cass, G.R., 1998. Source contributions to atmospheric fine carbon particle concentrations. Atmospheric Environment 32, 3805–3825.

Griffin, R.J., Nguyen, K., Dabdub, D., Seinfeld, J.H., 2003. A coupled hydrophobic-hydrophilic model for predicting secondary organic aerosol formation. Journal of Atmospheric Chemistry 44, 171–190.

Hughes, L.S., Allen, J.O., Bhave, P.V., Kleeman, M.J., Cass, G.R., Liu, D.Y., Fergenson, D.P., Morrical, B.D., Prather, K.A., 2000. Evolution of atmospheric particles along trajectories crossing the Los Angeles basin. Environmental Science and Technology 34, 3058–3068.

Hughes, L.S., Allen, J.O., Salmon, L.G., Mayo, P.R., Johnson, R.J., Cass, G.R., 2002. Evolution of nitrogen species air pollutants along trajectories crossing the Los Angeles area. Environmental Science and Technology 36, 3928–3935.

Junge, C.E., 1977. Basic considerations about trace constituents in the atmosphere as related to the fate of global pollutants. In: Suffet, I.H. (Ed.), Fate of Pollutants in the Air and Water Environments, Vol. 8, Part I, Wiley/Interscience, New York, pp. 7–26.

Kamens, R.M., Guo, Z., Fulcher, J.N., Bell, D.A., 1988. The influence of humidity, sunlight, and temperature on the daytime decay of polyaromatic hydrocarbons on atmospheric soot particles. Environmental Science and Technology 22, 103–108.

Kim, B.M., Tefferra, S., Zeldin, M.D., 2000. Characteristics of PM2.5 and PM10 in the south coast air basin of Southern California: Part I- spatial variations. Journal of Air and Waste Management Association 50, 2034–2044.

Kim, S., Shen, S., Zhu, Y., Hinds, W.C., Sioutas, C., 2002. Size distribution, diurnal and seasonal trends of ultrafine particles in source and receptor sites of the Los Angeles basin. Journal of Air and Waste Management Association 52, 174–185.

Lewtas, J., Yanbo, P., Derrick, B., Reimer, S., Eatough, D.J., Gundel, L.A., 2001. Comparison of sampling methods for semi-volatile organic carbon (SVOC) associated with PM2.5. Aerosol Science and Technology 3, 9–22.

Liang, C., Pankow, J.F., Odum, J.R., Seinfeld, J.H., 1997. Gas/particle partitioning of semivolatile organic compounds to model inorganic, organic, and ambient smog aerosols. Environmental Science and Technology 31, 3086–3092.

Lohmann, R.X., Harner, T., Thomas, G.O., Jones, K.C., 2000. A comparative study of the gas-particle partitioning of PCDD/Fs, PCBs, and PAHs. Environmental Science and Technology 34, 4943–4951.

Mader, B.T., Pankow, J.F., 2001. Gas/solid partitioning of semivolatile organic compounds (SOCs) to air filters. 2. Partitioning of polychlorinated dibenzodioxins polychlorinated dibenzofurans and polycyclic aromatic hydrocarbons to quartz fiber filters. Atmospheric Environment 35, 1217–1223.

Manchester-Neesvig, J.B., Schauer, J.J., Cass, G.R., 2003. The distribution of particle phase organic compounds in the atmosphere and their use for source apportionment during the southern California Children's Health Study. Journal of Air and Waste Management Association 53, 1065–1079.

Marr, L.C., Kirchstetter, T.W., Harley, R.A., Miguel, A.H., Hering, S.V., Hammond, S.K., 1999. Characterization of polycyclic aromatic hydrocarbons in motor vehicle fuels and exhaust emissions. Environmental Science and Technology 33, 3091–3099.

McMurry, P.H., Zhang, X.Q., 1989. Size distributions of ambient organic and elemental carbon. Aerosol Science and Technology 10, 430–437.

Meng, Z., Seinfeld, J.H., 1994. On the source of the submicrometer droplet mode of urban and regional aerosols. Environmental Science and Technology 20, 253–265.

Miguel, A.H., Kirchstetter, T.W., Harley, R.A., Hering, S.V., 1998. On-road emissions of particulate polycyclic aromatic hydrocarbons and black carbon from gasoline and diesel vehicles. Environmental Science and Technology 32, 450–455.

Mozurkewich, M., 1993. The dissociation constant of ammonium nitrate and its dependence on temperature, relative humidity and particle size. Atmospheric Environment 27A, 261–270.

Odum, J.T., Hoffmann, T., Bowman, F., Collins, T., Flagan, R.C., Seinfeld, J.H., 1996. Gas-particle partitioning and secondary organic aerosol yields. Environmental Science and Technology 30, 2580–2585.

Pankow, J.F., 1987. Review and comparative analysis of the theories on partitioning between the gas and aerosol particulate phases in the atmosphere. Atmospheric Environment 21, 2275–2283.

Pankow, J.F., 1994. An adsorption model of the gas/aerosol partitioning involved in the formation of secondary organic aerosol. Atmospheric Environment 28, 189–193.

Pankow, J.F., Bidleman, T.F., 1992. Effects of temperature *TSP* and per cent non-exchangeable material in determining the gas-particle partitioning of organic compounds. Atmospheric Environment 25A, 2241–2249.

Peters, A.J., Lane, D.A., Gundel, L.A., Northcott, G.L., Jones, K.C., 2000. A comparison of high volume and diffusion denuder samplers for measuring semivolatile organic compounds in the atmosphere. Environmental Science and Technology 34, 5001–5006.

Saxena, P., Hildemann, L.M., 1996. Water-soluble organics in atmospheric particles: a critical review of the literature and application of thermodynamics to identify candidate compounds. Journal of Atmospheric Chemistry 24, 57–109.

Schauer, J.J., 2003. Evaluation of elemental carbon as a marker for diesel particulate matter. Journal of Exposure Analysis and Environmental Epidimiology 13, 443–453.

Seinfeld, J.H., Pandis, S.N., 1998. In: Atmospheric Chemistry and Physics: From Air Pollution to Climate Changes. Wiley, New York, p. 41.

Seinfeld, J.H., Erdakos, G.B., Asher, W.E., Pakow, J.F., 2001. Modeling the formation of secondary organic aerosol: 2. The predicted effects of relative humidity on aerosol formation in the α-pinene-, β-pinene-, sabinene-, Δ3-carene-, and cyclohexene-ozone systems. Environmental Science and Technology 35, 1806–1817.

Turpin, B.T., Huntzicker, J.J., 1994. Investigation of organic aerosol sampling artifacts in the Los Angeles basin. Atmospheric Environment 28, 3061–3071.

Venkataraman, C., Friedlander, S.K., 1994. Size distributions of polycyclic aromatic hydrocarbons and elemental carbon. 2: Ambient measurements and effects of atmospheric processes. Environmental Science and Technology 28, 563–572.

Venkataraman, C., Thomas, S., Kulkarni, P., 1999. Size distributions of polycyclic aromatic hydrocarbons-gas/particle partitioning to urban aerosols. Journal of Aerosol Science 30, 759–770.

Wall, S.M., John, W., Ondo, J.L., 1988. Measurements for aerosol size distributions for nitrate and major ionic species. Atmospheric Environment 22, 1649–1656.

Wexler, A.S., Seinfeld, J.H., 1991. Second generation inorganic aerosol model. Atmospheric Environment 25A, 2731–2748.

Wolf, G.T., Ruthkosky, M.S., Stroup, D.P., Korsog, P.E., 1991. A characterization of the principal PM-10 species in Claremont (summer) and Long Beach (fall) during SCAQS. Atmospheric Environment 25A, 2173–2186.